BJP BRITISH JOURNAL OF PHARMACOLOGY

BPS BRITISH PHARMACOLOGICAL SOCIETY

British Journal of Pharmacology (2010), 160, 971–986

0007-1188/10
www.brjpharmacol.org

RESEARCH PAPER

The xanthine derivative KMUP-1 inhibits models of pulmonary artery hypertension via increased NO and cGMP-dependent inhibition of RhoA/Rho kinase

Hui-Hsuan Chung[1], Zen-Kong Dai[2], Bin-Nan Wu[3], Jwu-Lai Yeh[3], Chee-Yin Chai[4], Koung-Shing Chu[5], Chung-Pin Liu[1,6] and Ing-Jun Chen[3]

[1]*Institute of Medicine, Kaohsiung Medical University, Kaohsiung, Taiwan,* [2]*Department of Pediatrics, Kaohsiung Medical University, Kaohsiung, Taiwan,* [3]*Pharmacology, Kaohsiung Medical University, Kaohsiung, Taiwan,* [4]*Pathology, Kaohsiung Medical University, Kaohsiung, Taiwan,* [5]*Anesthesiology, Kaohsiung Medical University, Kaohsiung, Taiwan, and* [6]*Yuan's Hospital, Kaohsiung, Taiwan*

Background and purpose: KMUP-1 is known to increase cGMP, enhance endothelial nitric oxide synthase (eNOS) and suppress Rho kinase (ROCK) expression in smooth muscle. Here, we investigated the mechanism of action of KMUP-1 on acute and chronic pulmonary artery hypertension (PAH) in rats.

Experimental approach: We measured pulmonary vascular contractility, wall thickening, eNOS immunostaining, expressions of ROCK II, RhoA activation, myosin phosphatase target subunit 1 (MYPT1) phosphorylation, eNOS, soluble guanylyl cyclase (sGC), protein kinase G (PKG) and phosphodiesterase 5A (PDE-5A), blood oxygenation and cGMP/cAMP, and right ventricular hypertrophy (RVH) in rats.

Key results: In rings of intact pulmonary artery (PA), KMUP-1 relaxed the vasoconstriction induced by phenylephrine (10 μM) or the thromboxane A_2-mimetic U46619 (0.5 μM). In endothelium-denuded PA rings, this relaxation was reduced. In acute PAH induced by U46619 (2.5 $\mu g \cdot kg^{-1} \cdot min^{-1}$, 30 min), KMUP-1 relaxed vasoconstriction by enhancing levels of eNOS, sGC and PKG, suppressing those of PDE-5A, RhoA/ROCK II activation and MYPT1 phosphorylation, and restoring oxygenation in blood and cGMP/cAMP in plasma. Incubating smooth muscle cells from PA (PASMCs) with KMUP-1 inhibited thapsigargin-induced Ca^{2+} efflux and angiotensin II-induced Ca^{2+} influx. In chronic PAH model induced by monocrotaline, KMUP-1 increased eNOS and reduced RhoA/ROCK II activation/expression, PA wall thickening, eNOS immunostaining and RVH. KMUP-1 and sildenafil did not inhibit monocrotaline-induced PDE-5A expression.

Conclusion and implications: KMUP-1 decreased PAH by enhancing NO synthesis by eNOS, with consequent cGMP-dependent inhibition of RhoA/ROCK II and Ca^{2+} desensitization in PASMCs. KMUP-1 has the potential to reduce vascular resistance, remodelling and RVH in PAH.

British Journal of Pharmacology (2010) **160,** 971–986; doi:10.1111/j.1476-5381.2010.00740.x

Keywords: KMUP-1; pulmonary hypertension; eNOS; RhoA; Rho Kinase; cGMP

Abbreviations: ANG II, angiotensin II; eNOS, endothelium nitric oxide synthase; ER, endoplasmic reticulum; MLCP, myosin light chain phosphatase; MYPT1, myosin phosphatase target subunit 1; PA, pulmonary artery; PAH, pulmonary artery hypertension; PASMCs, pulmonary artery smooth muscle cells; PDE-5A, phosphodiesterase-5A; PKG, protein kinase G; ROCK, Rho kinase; ROCK II, Rho kinase II; RVH, right ventricular hypertrophy; sGC, soluble guanylate cyclase; TG, thapsigargin; TXA_2, thromboxane A_2

Introduction

Pulmonary artery hypertension (PAH) is a severe and fatal disease. Sildenafil, inhibitors of Rho kinase (ROCK) and statins have been used to treat PAH. Because the xanthine

Correspondence: Dr Ing-Jun Chen, Department of Pharmacology, Faculty of Medicine, Kaohsiung Medical University, 100 Shih-Chuan 1st Road, Kaohsiung 807, Taiwan. E-mail: ingjun@kmu.edu.tw
Received 6 October 2009; revised 4 January 2010; accepted 30 January 2010

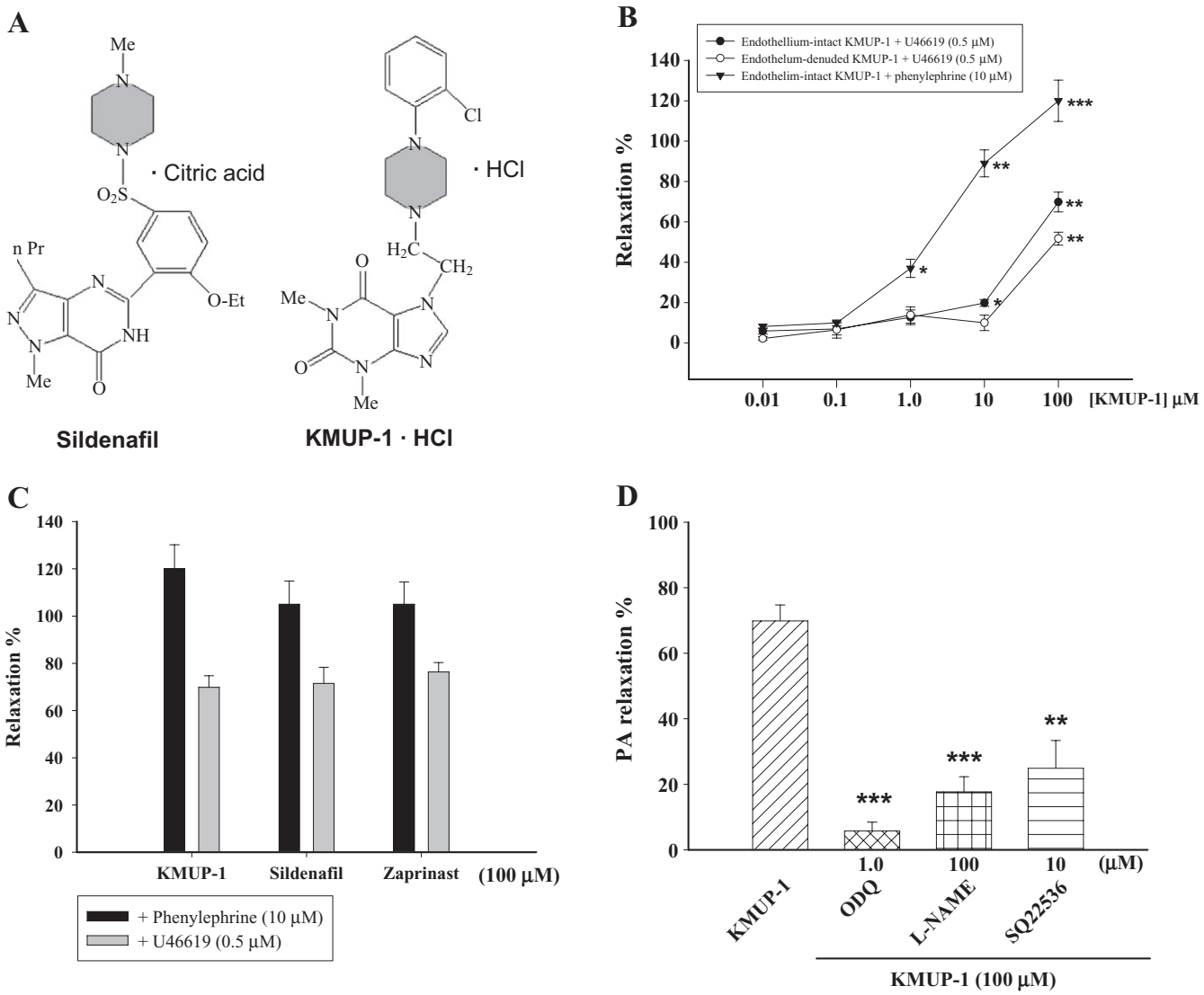

Figure 1 Chemical structure of KMUP-1 and sildenafil, and inhibition of PA constriction. (A) KMUP-1 hydrochloride (KMUP-1·HCl) and sildenafil citrate; (B) Relaxation of KMUP-1 (0.01–100 μM), constricted by phenylephrine (10 μM) and U46619 (0.5 μM) in endothelium-intact or -denuded PA; (C) KMUP-1, sildenafil and zaprinast at 100 μM inhibited phenylephrine (10 μM)- and U46619 (0.5 μM)-induced PA constriction; and (D) pretreatment with ODQ (1.0 μM), L-NAME (100 μM) and SQ22536 (10 μM) in organ bath decreased KMUP-1 (100 μM)-induced relaxation against U46619 (0.5 μM)-induced PA constriction. Values are expressed as means ± s.e., $n = 6$, $^*P < 0.05$; $^{**}P < 0.01$ phenylephrine or U46619 versus +KMUP-1. L-NAME, N^{ω}-nitro-L-arginine methyl ester; ODQ, 1*H*-[1,2,4]oxadiazolo[4,3-*a*]quinoxalin-1-one; PA, pulmonary artery.

derivative KMUP-1 (Figure 1A) raises cGMP levels (as does sildenafil), increases levels and activity of endothelial nitric oxide synthase (eNOS) and suppresses ROCK in smooth muscle (Wu *et al*., 2006; Liu *et al*., 2007), we postulated that this compound would ameliorate PAH.

Pulmonary vasoactive mediators, including nitric oxide (NO), prostacyclin, endothelin-1, 5-HT, chemokines, thromboxane A_2 (TXA_2) and hypoxia are involved in severe PAH (Bohm and Pernow, 2007; Ni *et al*., 2008). In experimental models, the TXA_2-mimetic U46619, given i.v., causes acute PAH and i.p. monocrotaline causes chronic PAH, accompanied by medial wall thickening of pulmonary artery (PA), endothelium rarefaction, sustained PA vasoconstriction and other consequences such as right ventricular hypertrophy (RVH) and liver toxicity (Copple *et al*., 2003; Lamberts *et al*., 2007; Homma *et al*., 2008). Using both the acute model of PAH induced by U46619 and the chronic monocrotaline model of PAH in rats, we assessed if KMUP-1 treatment would inhibit PAH, via cGMP-dependent inhibition of RhoA/ROCK II in PA and lung tissue.

RhoA-dependent Ca^{2+} sensitization of vasculature, including that caused by inhibition of myosin light chain phosphatase (MLCP) in PA, is an important factor in sustained vasoconstriction. ROCK-dependent MLCP inhibition is responsible for both RhoA-dependent Ca^{2+} sensitization and agonist-induced stimulation in smooth muscle cells (Sauzeau *et al*., 2000). This inhibition is brought about by phosphorylation of myosin phosphatase target subunit 1 (MYPT1) at

Thr-696 by ROCK, leading to Ca^{2+} sensitization and smooth muscle contraction (Feng *et al*., 1999). Conversely, vascular smooth muscle relaxation can result from a decrease in cytosolic Ca^{2+} concentration and/or reduced Ca^{2+} sensitivity of the contractile apparatus. Endogenous NO raises levels of cGMP, relaxing vascular smooth muscle and enlarging the vessel lumen, leading to increased expression of protein kinase G (PKG). The vasodilator action of the cGMP/PKG pathway also decreases cytosolic Ca^{2+} and causes Ca^{2+} desensitization by increased MLCP activity (Sauzeau *et al*., 2000).

PAH is regulated by NO-induced vasodilatation and cell proliferation in PA, characterized by increased vascular pressure, and progressive structural remodelling and associated RVH (Puchalski *et al*., 2006). NO signalling includes the activation of soluble guanylate cyclase (sGC) and the subsequent generation of cGMP as a second messenger to produce vasodilation. NO maintains vessel homeostatic functions and ameliorates pathological changes such as PA over-contraction and smooth muscle cell proliferation that would lead to increased PA resistance and obstruction (McLaughlin and McGoon, 2006). The pathogenesis of PAH involves increased production of TXA_2 (Cogolludo *et al*., 2003), reduction of pulmonary eNOS and increased RhoA/ROCK in the PA (Bohm and Pernow, 2007). The loss of the endothelium-derived NO may be due to reduced production of NO caused by down-regulated eNOS and up-regulated RhoA/ROCK in hypoxic PAH (Takemoto *et al*., 2002).

Inhibition of ROCK may be of benefit in PAH by restoring PKG-mediated vasodilatation in hypoxia (Gao *et al*., 2007). The ROCK inhibitors Y27632 and fasudil have been used to treat PAH (Fukumoto *et al*., 2005). RhoA/ROCK may serve as a point of convergence of various signalling cascades in PAH, including the cGMP/PKG pathway (Oka *et al*., 2007). By raising levels of cGMP, ROCK can be inhibited, which is why sildenafil can improve PAH. Moreover, statins increase eNOS mRNA stability by inhibiting Rho GTPases, including RhoA, to increase the production and bioavailability of endothelium-derived NO (Kosmidou *et al*., 2007). cGMP-dependent inhibition of RhoA/ROCK has a similar pleitropic effect to statins.

Regulation of upstream eNOS/sGC, downstream RhoA/ROCK II and phosphodiesterase-5A (PDE-5A) in the cGMP pathway affects vascular contractility and resistance (Oka *et al*., 2007; Kirsch *et al*., 2008). NO synthesized by eNOS can relax vascular smooth muscles by increasing cGMP and suppressing RhoA/ROCK II expression. Furthermore, inhibition of PDE-5A by sildenafil can enhance this NO-derived contribution, by preserving cGMP. In contrast, increased PDE-5 activity could contribute to the pathophysiology of PAH (Deruelle *et al*., 2005).

In this context, we tested whether the actions of KMUP-1 may offer the advantage of the same compound simultaneously enhancing eNOS and suppressing RhoA/ROCK II, in order to relax the PA and thus inhibit PAH. To elucidate the mechanism of action, we measured the co-localized expression of eNOS, sGC, cGMP, PKG, PDE-5A and ROCK II, phosphorylation of MYPT1 and activation of RhoA in PA of acute PAH. The effects of KMUP-1 on these variables would provide an estimate of the applicability of such treatment for inhibiting chronic PAH.

Methods

Animals

All animal care and the experimental protocols of this study were approved by the Animal Care and Use Committee of the Kaohsiung Medical University. Male Wistar rats (200–250 g) provided by the National Laboratory Animal Breeding and Research Center (Taipei, Taiwan) were housed under constant temperature and controlled illumination. Food and water were available *ad libitum*.

Haemodynamic measurements

Wistar rats weighing 300–350 g were anaesthetized with pentobarbital sodium (40 $mg \cdot kg^{-1}$, i.p.). Following tracheal cannulation, anaesthetized rats were mechanically ventilated; the femoral artery was cannulated for continuous monitoring of mean arterial blood pressure (MABP) and heart rates (HR). Mean PA pressure (MPAP) was measured in the PA of open-chest rats. Haemodynamic parameters were recorded with a pressure transducer (Gould, Model P50, Oxnard, CA, USA). A femoral vein was cannulated for administration of KMUP-1 and other drugs. A heating pad was used to maintain a body temperature of 37°C.

U46619- and monocrotaline-induced PAH

To reduce acute PAH and vasoconstriction-induced hypoxia, we intravenously infused KMUP-1. In these experiments, rats were anaesthetized, and KMUP-1 (0.5–2.0 $\mu g \cdot kg^{-1} \cdot min^{-1}$, 20 min, i.v.), sildenafil (1.0 $\mu g \cdot kg^{-1} \cdot min^{-1}$, i.v.) or zaprinast (10 $\mu g \cdot kg^{-1} \cdot min^{-1}$, i.v.) were administered, followed by intravenous infusion of U46619 (2.5 $\mu g \cdot kg^{-1} \cdot min^{-1}$, i.v, 30 min), to achieve acute PAH. MPAP, MABP and HR were continuously recorded.

In the chronic PAH model, 8 week old adult Wistar rats were given a single injection of monocrotaline (60 $mg \cdot kg^{-1}$, i.p.) on day 0. A single i.p. injection of monocrotaline (60 $mg \cdot kg^{-1}$) induces severe PAH, associated with the development of PAH within 3 weeks and a subsequent high mortality rate in rats (Abe *et al*., 2004). Daily oral (5 $mg \cdot kg^{-1}$) and i.p. (1 $mg \cdot kg^{-1}$) administration of KMUP-1 from day 1 to day 21 was used to reduce chronic PAH and associated remodelling or hyperplasia. On day 21, rats were anaesthetized, and MPAP, MABP and HR were recorded as mentioned above. Lung tissues were then removed for Western blotting and immunohistochemistry.

PA rings and tension measurements

Wistar rats were given an overdose of pentobarbital sodium (60 $mg \cdot kg^{-1}$, i.p.), then underwent open-chest surgery. During surgery, a thoracic retractor was used to help isolation of PA. The chest was opened to dissect the second branches of the main PA, which were cut into 2–3 mm rings, suspended under isometric conditions and connected to a force transducer as previously described (Ugo Basile, Model 7004, Comerio-VA, Italy) (Schach *et al*., 2007). In some experiments, the endothelium was denuded mechanically by inserting the tweezers into the lumen and rolling the PA ring back and forth five

times. The experiment measured the response to constriction caused by the TXA_2 receptor agonist U46619 (0.5 μM) and α-adrenoceptor agonist phenylephrine (10 μM). The preparation of PA rings was stretched to a basal tension of 1 g and allowed to equilibrate for 60–90 min. After equilibration, PA rings were constricted with U46619 or phenylephrine. Once the contractile response to each agonist had reached a stable tension, KMUP-1 (0.01–100 μM) was added to the organ bath for 50 min. The percentage of relaxation was estimated using the following equation: relaxation (%) = (maximal contraction – relaxation level)/(maximal contraction – basal level) × 100. Data were obtained from U46619 or phenylephrine-induced maximal contractile responses in PA, treated with KMUP-1 or the PDE-5 inhibitors, sildenafil and zaprinast. The EC_{50} value of KMUP-1, sildenafil and zaprinast was estimated by the concentration required to produce 50% relaxation against phenylephrine (10 μM)- and U46619 (0.5 μM)-induced maximal constriction. Contractile tension and estimation of EC_{50} were carried out by a computer-based program.

Experiments were performed to investigate the mechanisms underlying the PA relaxation by KMUP-1. The relaxant effects of KMUP-1 were tested in PA rings pretreated with the sGC inhibitor 1*H*-[1,2,4]oxadiazolo[4,3-*a*]quinoxalin-1-one (ODQ; 1.0 μM), the NOS inhibitor N^{ω}-nitro-L-arginine methyl ester (L-NAME; 100 μM) or the adenylate cyclase inhibitor SQ22536 (10 μM) before U46619 (0.5 μM) was added to produce a maximal contraction. SQ 22536 (10 μM) was used to test the involvement of cAMP production in PA relaxation.

Preparation of pulmonary arterial smooth muscle cells

Rats were anaesthetized with a lethal dose of pentobarbital sodium (60 $mg \cdot kg^{-1}$, i.p.), and the skin was sterilized with 75% alcohol. The chest was opened, and the heart and lungs were removed. The organs were rinsed several times in phosphate buffer solution (PBS). The PAs were segregated in a sterile manner, the outer sphere was peeled, the microtubule was snipped visually and endothelium was shaved slightly 2–3 times to remove endothelial cells. The tunica media was prepared in scraps (1 mm^3) in Dulbecco's modified Eagle's medium (DMEM). Pulmonary arterial smooth muscle cells (PASMCs) were cultured in DMEM containing 10% fetal bovine serum (5% CO_2 at 37°C) (Gao *et al*., 2007). The culture medium was changed every 3 days, and cells were subcultured to confluence. Primary cultures of two to four passages were used in the experiments. Cells were examined by immunofluorescence staining of α-actin to confirm the purity of PASMCs. Over 95% of the cell preparation was found to be composed of smooth muscle cells.

Protein expression by Western blotting analysis

The second branches of the main PA were isolated, cut into 2–3 mm strips and incubated with KMUP-1 (10 μM) for 60, 90 and 120 min to measure changes in eNOS, ROCK and PDE-5A protein expression, compared with controls. To measure effects of KMUP-1 on eNOS, sGC, PKG, PDE-5A, ROCK II expression, MYPT1 phosphorylation and RhoA inactivation, the PA rings were incubated with or without KMUP-1 (1.0–100 μM) for 90 min; another group was then treated with U46619 (0.5 μM) for 30 min after KMUP-1 administration at 60 min. Untreated wells were used as controls. To explore the mechanism of action, the rings were pretreated with the eNOS inhibitor L-NAME (100 μM), sGC inhibitor ODQ (1.0 μM) or the PKG antagonist. Rp-8-Bromo-β-phenyl-1, N^2-ethenoguanosine 3′ : 5′-cyclic mono-phosphorothioate (Rp-8-Br-PET-cGMPS; 1.0 μM) for 10 min before KMUP-1 was applied following the same procedure mentioned above. Whole right lung tissues of monocrotaline-treated rats were isolated and cut into small chips to extract protein. To measure protein expression levels, the total proteins were extracted, and Western blotting analyses were performed as described previously (Wu *et al*., 2006). Mouse or rabbit monoclonal antibodies to eNOS (Upstate, Lake Placid, NY, USA), sGCα (Sigma-Aldrich, Saint Louis, CA, USA), sGCβ (UC, Santa Cruz, CA, USA), PDE-5A (BD Tansduction, San Jose, CA, USA), PKG (Calbiochem, San Diego, CA, USA), ROCK II (Upstate), RhoA (UC), MYPT-1 (Upstate), phospho-MYPT-1 (Thr-696) (Upstate) and the loading control protein β-actin (Sigma-Aldrich, St. Louis, MO, USA) were used in the Western blot analyses. The isolated PA rings were put into extraction buffer (Tris 10 mM, pH 7.0, NaCl 140 mM, phenylmethylsulphonyl fluoride 2 mM, dithiothreitol 5 mM, NP-40 0.5%, pepstatin A 0.05 mM and leupeptin 0.2 mM), cut into small chips and then centrifuged at 12 500× *g* for 30 min. The protein extract was then boiled in a ratio of 5:1 with sample buffer (Tris 100 mM, pH 6.8, glycerol 20%, sodium dodecyl sulphate (SDS) 4% and bromophenol blue 0.2%). Electrophoresis was performed using 10% SDS-polyacrylamide gel (2 h, 100 V, 40 mA, 20 μg protein per lane). Separated proteins were transferred to PolyVinyliDene Fluoride membranes treated with 5% fat-free milk powder to block the nonspecific IgGs (90 min, 100 V) and incubated for 2 h with specific antibody. The blot was then incubated with anti-mouse or anti-goat IgG linked to alkaline phosphatase (1:1000) for 1 h. Immunoreactive bands were visualized using horseradish peroxidase-conjugated secondary antibodies and subsequent enhanced chemiluminescent (ECL) detection.

Measurement of cellular cGMP and cAMP

Cultured PASMCs were incubated with KMUP-1 (10 μM) or zaprinast (10 μM) in incubation plate wells for 24 h and terminated by adding 10% trichloroacetic acid (TCA). Cell suspensions were sonicated and centrifuged at 2500 g for 15 min at 4°C. To remove TCA, the supernatants were extracted three times with five volumes of water-saturated diethyl ether. The supernatants were then lyophilized. To measure pulmonary release of cGMP and cAMP, pulmonary arterial blood was collected in sample tubes coated inside with traces of heparin. The mixture was centrifuged at 4°C (210× *g*, 15 min) to obtain the plasma. cGMP and cAMP in pulmonary arterial plasma and PASMCs were determined by radioimmunoassay using an acetylated [^{125}I]-cGMP and [^{125}I]-cAMP assay kit respectively (GE Healthcare, Little Chalfont, Buckinghamshire, UK).

Intracellular calcium concentration $[Ca^{2+}]_i$

The measurement of $[Ca^{2+}]_i$ in PASMCs was performed using a spectroflurophotometer as previously reported (Wang *et al*.,

2004). PASMCs, cultured for two to four passages and resuspended by trypsin, were loaded with Fura-2/acetoxymethyl to permit the measurement of $[Ca^{2+}]_i$ changes of cells within cuvettes by spectroflurophotometry (Shimadzu, RF-5301PC, Kyoto, Japan). KMUP-1 or Y27632 was applied before angiotensin II (ANG II, 1.0 μM) or thapsigargin (TG, 1.0 μM) was added. Endoplasmic reticulum (ER) Ca^{2+}ATPase is inhibited by TG, leading to depletion of Ca^{2+} stores (Sauzeau *et al*., 2000).

Acute hypoxia and blood oxygenation

To confirm that intravenous U46619 leads to acute hypoxia, blood samples were simultaneously obtained from femoral arteries at the end of the injection. This was followed by pretreatment with intra-peritoneal injection and intravenous infusion of KMUP-1 and reference agents before administration of U46619. After pretreatment with KMUP-1 and the administration of U46619, blood was sampled through the catheter and analysed by an automatic blood gas analyser (AVL OMNI™, Nutley, NJ, USA). The analyses included the measurement of arterial oxygen pressure (PaO_2). PaO_2 values were compared with non-treatment values.

RhoA activity

RhoA activity is indicated by the translocation of RhoA from cytosol to the membrane. Tissue extracts were separated into cytosol, nuclear and membrane (CNM) fractions. To assess the effects of KMUP-1 and vehicle on translocation of RhoA in PA, cytosol and membrane proteins were extracted from U46619-treated PA rings for analyses of RhoA expression. To assess RhoA activity in tissue, control and monocrotaline-treated rat lungs were extracted using a CNM kit (Chemicon International Inc., Billerica, MA, USA) as previously reported (Korn *et al*., 2005). RhoA protein in membrane and cytosolic fractions was determined by standard Western blot analysis using mouse monoclonal anti-RhoA antibody (UC). Immunoreactive bands were visualized using horseradish peroxidase-conjugated secondary antibodies and subsequent ECL detection. RhoA activity was presented as the ratio of RhoA protein in the membrane/cytosolic fractions (Homma *et al*., 2007).

Morphologic and immunohistochemical analyses

To confirm the vascular hyperplasia in PA rings, lung tissue sections from rats treated with monocrotaline were prepared as previously described and stained with haematoxylin-eosin (Hongo *et al*., 2000). Microphotographic measurement of PA in the lung sections was performed using a colour digital camera mounted on a computer-interfaced light microscope (Eclipse TE2000-S microscope, Nikon, Tokyo, Japan) interfacing with a NIS-Elements F 3.0 software (Tokyo, Japan). PA wall thickness was measured as the distance between the external and internal elastic laminae of each artery, and the distance was measured using an Image J software analysis system (Oxnard, CA, USA). The percent PA wall thickness (%) of each artery was calculated using the following formula: PA wall thickness (%) = (2 × medial wall thickness)/(external diameter) × 100. The average of six measurements of PA in each animal was used in our analysis. Assessment of RVH was made from the weight ratio of right ventricular wall area to left ventricular wall area plus septum, the (RV/(LV + S) ratio.

Although Western blotting indicated that KMUP-1 increased eNOS expression, immunohistochemical evidence was needed to confirm this. In this study, the immunohistochemical analysis of increased eNOS induced by KMUP-1 was performed as follows. The lungs were perfused with saline followed by 10% formalin and then placed in 10% formalin for paraffin embedding. The lung tissues were cut into 3–5 μm sections on slides, de-waxed in 100% xylene, and then rehydrated in graded alcohol solutions. Throughout the procedure, slides were washed as appropriate in PBS. Antigen retrieval was performed by microwave treatment for eNOS immunostaining. Sections were treated with 3% H_2O_2 (10 min) to inhibit endogenous peroxidases and incubated with normal serum (60 min) to reduce non-specific binding of secondary antibodies. Sections were then incubated at 4°C overnight with eNOS antibodies. After washing off unbound primary antibodies, sections were incubated with secondary biotinylated antibodies against mouse or rabbit (DAKO Co., Tokyo, Japan) (60 min), followed by incubation in avidin/biotin/horseradish peroxidase complex (DAKO Co.) (30 min). Subsequently, peroxidase activity was visualized by incubation (3 min) with 0.05% 3,3′-diaminobenzidine (DAKO Co.), which gives a brown reaction product. The reaction was stopped by washing with water. The slides were counterstained with haematoxylin.

Statistical evaluation of data

The results are expressed as means ± s.e. Statistical differences were determined by independent and paired Student's *t*-test in unpaired and paired samples respectively. Whenever a control group was compared with KMUP-1 and other treated groups, the one-way ANOVA or two-way repeated measures ANOVA was used. When the ANOVA showed a statistical difference, Dunnett's or Student–Newman–Keuls test was applied. A *P*-value less than 0.05 was considered to be significant in all experiments. Analysis of the data and plotting of the figures were done with SigmaPlot software (Version 8.0, SPSS Scientific, Chicago, IL, USA) and SigmaStat (Version 2.03, SPSS Scientific) run on an IBM-compatible computer.

Materials

KMUP-1was synthesized in our laboratory. In brief, theophylline was reacted with dichloroethane and then reacted with 2-chlorophenylpiperazine to obtain KMUP-1, which was re-crystallized from the solvent mixture of ethanol and 1N HCl. The melting point of the compound was 249–252°C. We were unable to further raise the melting point, indicating that this was the highest purity of KMUP-1 (99.9%), confirmed by high performance liquid chromatography. 5-[2-ethoxy-5-(4-methylpiperazin-1-yl)sulfonylphenyl]-1-methyl-3-propyl-4H-pyrazolo[4,3-d]pyrimidin-7-one (sildenafil) was supplied by the Cadila Healthcare Ltd. (Maninagar, India). (*R*)-(+)-*trans*-4-(1-aminoethyl)-N-(4-pyridyl) cyclohexanecarboxamide dihydrochloride monohydrate (Y27632), 1,4-dihydro-5-(2-propoxyphenyl)-7H-1,2,3-triazolo(4,5-d)pyrimidin-7-one

Table 1 Estimated EC_{50} values for KMUP-1, sildenafil and zaprinast in inhibiting phenylephrine (PE)- and U46619-induced PA constriction

Compound	*EC_{50} (μM)*	
	PE	*U46619*
KMUP-1	1.0 ± 0.1	38 ± 4
Sildenafil	0.59 ± 0.07	21 ± 2
Zaprinast	3.9 ± 0.4	1.1 ± 0.1

Data in the table are means ± SEM from $n = 6$ experiments. Rings of pulmonary artery were contracted by PE (10 μM) or U46619 (0.5 μM).

(zaprinast), ODQ, L-NAME, 9-(terahydro-2-furanyl)-9H-purin-6-amine (SQ22536), 9,11-Dideoxy-11α,9α-epoxymethano prostaglandin $F_{2\alpha}$ (U46619) (3R, 4R, 5R, 13aR, 13bR) - 4, 5 - dihydroxy - 3, 4, 5 - trimethyl - 4, 5, 8, 10, 12, 13, 13a, 13b - octahydro - 2H - [1, 6] dioxacycloundecino [2, 3, 4 - gh] pyrrolizine-2,6(3H)-dione (monocrotaline), Rp-8-Bromo-β-phenyl - 1, N^2 - ethenoguanosine 3′ : 5′ - cyclic mono - phosphorothioate hydrate sodium salt (Rp-8-Br-PET-cGMPS), [(3S,3aR,4S,6S,6aR, 7S,8S,9bS)-6-acetyloxy-4-butanoyloxy-3, 3a - dihydroxy - 3, 6, 9 - trimethyl - 8 - [(Z) - 2 - methylbut - 2 - enoyl]oxy-2-oxo-4,5, 6a,7,8,9b-hexahydroazuleno [4,5-b] furan-7-yl] octanoate (TG) and ANG II were purchased from Sigma-Aldrich. Drug/molecular target nomenclature follows Alexander *et al*. (2009).

Results

Inhibition of phenylephrine- and U46619-induced vasoconstriction

Phenylephrine (10 μM)-induced PA constriction was concentration-dependently inhibited by KMUP-1 (0.01–100 μM). KMUP-1 relaxed U46619-induced constriction in endothelium-intact PA rings, and this relaxation is significantly reduced in endothelium-denuded PA rings. KMUP-1-induced vasorelaxation is more likely to be endothelium dependent (Figure 1B). Particularly, KMUP-1 at 100 μM could reduce phenylephrine-induced maximal constriction to below baseline. KMUP-1, sildenafil and zaprinast at 100 μM all significantly relaxed phenylephrine (10 μM)- and U46619 (0.5 μM)-induced maximal contraction (Figure 1B), but these effects were not significantly different from each other (Figure 1C). The EC_{50} of KMUP-1 inhibition against PE- and U46619-induced maximal constriction was estimated and is shown in Table 1. Pretreatment of PA rings with the sGC inhibitor ODQ (1.0 μM) and the NOS inhibitor L-NAME (100 μM) decreased the relaxation of U46619-induced contractions by KMUP-1 (100 μM). Pretreatment with the adenylyl cyclase inhibitor SQ22536 (10 μM) also reduced relaxation by KMUP-1 (Figure 1D).

Acute enhancement of eNOS expression and suppression of PDE-5A/ROCK II

After incubation of KMUP-1 (10 μM) with PA rings for 60, 90 and 120 min, eNOS expression in the rings was up-regulated, and ROCK II and PDE-5A were down-regulated in a time-dependent manner (Figure 2).

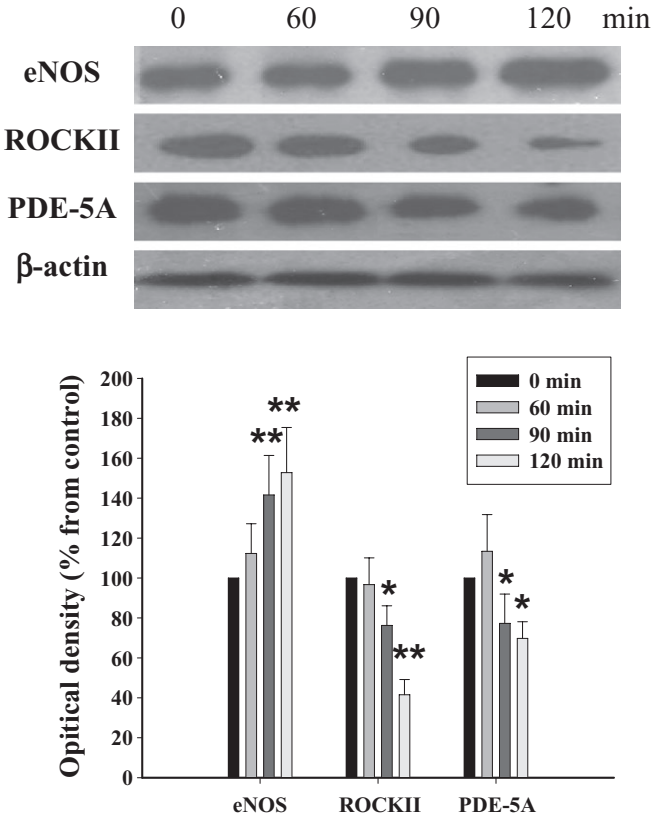

Figure 2 Time-dependent changes in expression of eNOS, ROCK II and PDE-5A in PA rings treated with KMUP-1. Incubation of KMUP-1 (10 μM) with PA rings altered the expression of eNOS, ROCK II and PDE-5A, respectively, at 60, 90 and 120 min. Values are expressed as means ± s.e., $n = 6$, $^*P < 0.05$; $^{**}P < 0.01$ versus time 0. eNOS, endothelial nitric oxide synthase; PA, pulmonary artery; PDE-5A, phosphodiesterase-5A; ROCK II, Rho kinase II.

Co-localized eNOS/sGCα/cGCβ/PKG expression, MYPT1 phosphorylation and RhoA activation

Incubation of KMUP-1 (100 μM) with PA rings for 90 min significantly increased expression of eNOS, sGCα, cGCβ and PKG, and decreased expression of PDE-5A and ROCK II in the absence of U46619 (Figure 3A). Incubation of KMUP-1 (100 μM) with PA ring for 60 min, followed by the addition of U46619 (0.5 μM) for 30 min, significantly increased expression of eNOS, sGCα, sGCβ, and PKG, and decreased expression of PDE5A or ROCK II (Figure 3B). Although incubation with U46619 alone increased expression of ROCK II and PDE-5A, it did not significantly affect expression of eNOS, sGCα, sGCβ or PKG in PA rings. In the absence or presence of U46619 (0.5 μM) in PA rings, KMUP-1 (1.0–100 μM) decreased RhoA translocation from cytosol to membrane and concentration-dependently decreased the membrane/cytosol ratio or RhoA activity under both conditions in PA rings (Figure 3C,D). Incubation with U46619 (0.5 μM) for 30 min induced MYPT1 phosphorylation, and this phosphorylation

was prevented by pre-incubation with KMUP-1 (10 μM) for 60 min before adding U46619 (Figure 3E).

Down-regulation of ROCK II via PKG

ROCK II expression in PA rings was decreased by KMUP-1 (10 μM), and this decrease was reversed by pretreatment with L-NAME (100 μM) or ODQ (1.0 μM) (Figure 4A). Incubation with KMUP-1 or the ROCK inhibitor Y27632 decreased the expression of ROCK II. However, pretreatment with the PKG inhibitor Rp-8-Br-PET-cGMPS (1.0 μM) reversed this suppression of ROCK II (Figure 4B).

Increases of cGMP and cAMP

Intravenous U46619 (2.5 $\mu g \cdot kg^{-1} \cdot min^{-1}$, 30 min) alone had no significant effect on plasma cGMP or cAMP in pulmonary blood samples from rats. However, when intravenous KMUP-1 (0.5–2 $\mu g \cdot kg^{-1} \cdot min^{-1}$, 20 min) was followed by U46619 infusion, there was a dose-dependent increase in pulmonary plasma cGMP, significantly greater than the increase in cAMP levels, compared with controls (Figure 5A). Increase of cGMP ($P < 0.01$) was more marked than the increase of cAMP ($P < 0.05$) in plasma, at the higher doses of KMUP-1 (1–2 $\mu g \cdot kg^{-1} \cdot min^{-1}$). In PASMCs, KMUP-1 (10 μM) increased the accumulation of cGMP more than it increased cAMP, compared with controls. Notably, KMUP-1 or zaprinast both increased cGMP almost threefold compared with basal control values ($P < 0.01$). The PDE-5 inhibitor zaprinast (10 μM) also increased cGMP, but not cAMP (Figure 5B).

Ca^{2+} mobilization of PASMCs

Figure 6A shows the changes of $[Ca^{2+}]i$ in fura-2-loaded and Ca^{2+}-free PASMCs in the presence of 1.0 μM TG, an inhibitor of ER membrane Ca^{2+}ATPases. TG increased $[Ca^{2+}]_i$ levels (mean values 91 ± 13–177 ± 10 nM) in PASMCs, indicating Ca^{2+} efflux from the ER to the cytosol. Pretreatment with KMUP-1 (10 μM) and Y27632 (10 μM) inhibited this elevation (89 ± 10–122 ± 22 nM and 95 ± 1.5–118 ± 23 nM respectively) (Figure 6A, left panel). KMUP-1 and Y27632 altered ANG II-induced increase of $[Ca^{2+}]_i$ in buffer containing Ca^{2+} (Figure 6B, left panel). KMUP-1 inhibited ANG II-induced increase in $[Ca^{2+}]i$ significantly more than Y27632 (Figure 6B). Thus, KMUP-1, like Y27632, significantly inhibited increases in $[Ca^{2+}]_i$ induced by TG or ANG II.

Acute PAH and U46619

Intravenous infusion of U46619 for 30 min produced a significant increase in MPAP, which was reduced by pretreatment with KMUP-1. Intravenous KMUP-1 (0.5–2.0 $\mu g \cdot kg^{-1} \cdot min^{-1}$, 20 min) dose-dependently decreased MPAP (Figure 7A). Infusion of KMUP-1 (1.0 $\mu g \cdot kg^{-1} \cdot min^{-1}$, 20 min), sildenafil citrate (1.0 $\mu g \cdot kg^{-1} \cdot min^{-1}$, 20 min) or zaprinast (10 $\mu g \cdot kg^{-1} \cdot min^{-1}$, 20 min) all decreased U46619-induced rises in MPAP (Figure 7B). KMUP-1 (0.5–1.0 $\mu g \cdot kg^{-1} \cdot min^{-1}$) infused alone did not significantly affect MABP compared with the basal level (Figure 7C).

Acute hypoxia and U46619

As shown in Table 2, the infusion of U46619 (2.5 $\mu g \cdot kg^{-1} \cdot min^{-1}$ 30 min, i.v.) decreased PaO_2 in the blood of Wistar rats compared with controls. There was no significant change of pH and P_{CO2} values after treatment with U46619 (data not shown). However, pretreatment with KMUP-1 (1.0 $\mu g \cdot kg^{-1} \cdot min^{-1}$, 20 min, i.v.) decreased U46619-induced reduction of Pa_{O2}, bringing it back to near-normal levels. U46619-induced reduction of PaO_2 was also restored by sildenafil (1.0 $\mu g \cdot kg^{-1} \cdot min^{-1}$, 20 min, i.v.) and by zaprinast (10 $\mu g \cdot kg^{-1} \cdot min^{-1}$, 20 min, i.v.).

Chronic PAH, vascular remodelling and RVH

Rats treated with vehicle once a day for 21 days after a single intra-peritoneal injection of monocrotaline developed PAH along with marked increases in PA wall thickness, as demonstrated by morphological measurements and estimated MPAP and RV/(LV + S) ratio, reflecting the development of RVH, compared with controls. Daily treatment with KMUP-1 (5 $mg \cdot kg^{-1} \cdot day^{-1}$ p.o. or 1 $mg \cdot kg^{-1} \cdot day^{-1}$ i.p.) for 21 days significantly reduced monocrotaline-induced increases in MPAP, RV/LV + S and PA wall thickness (Table 3). KMUP-1 was clearly able to reduce monocrotaline-induced PAH, while MABP and HR were unaffected in monocrotaline-treated rats.

Sustaining eNOS, sGC, RhoA and ROCK II, and augmenting PDE-5A expression

In the lung tissue of monocrotaline-treated rats, Western blotting analysis demonstrated that expression of eNOS and sGCα decreased and ROCK II expression increased (Figure 8A). In monocrotaline-treated rats given KMUP-1 (5 $mg \cdot kg^{-1} \cdot day^{-1}$, p.o. or 1 $mg \cdot kg^{-1} \cdot day^{-1}$, i.p., 21 days), lung eNOS and sGCα were higher than that in rats receiving monocrotaline only. Oral or i.p. administration of KMUP-1 also inhibited monocrotaline-induced expression of ROCK (Figure 8A). Studies of the distribution of RhoA between membranes and cytosol in lung extracts (Figure 8B) showed that the membranes of monocrotaline-treated lungs had higher RhoA expression than those from untreated (control) rats. Adding KMUP-1 (p.o. or i.p) significantly reduced this raised expression of RhoA (Figure 8B). Expression of PDE-5A in lung tissue was increased by monocrotaline, but neither KMUP-1 nor sildenafil, given for 21 days, reduced this raised level of PDE-5A expression. Surprisingly, both treatments increased PDE-5A levels even further (Figure 8C). Note that in U46619-treated PA rings, expression of PDE-5A was inhibited by KMUP-1 (Figure 3).

Morphology and quantitative eNOS immunohistochemistry

Twenty-one days after monocrotaline injection, marked increases of PA wall thickness were found compared with those in lungs of normal rats. Long-term treatment with KMUP-1 (5 $mg \cdot kg^{-1} \cdot day^{-1}$, p.o. and 1 $mg \cdot kg^{-1} \cdot day^{-1}$, i.p. for 21 days) after the injection of monocrotaline reduced the wall thickness and muscularization of the PA (Figure 9A and Table 3). Immunohistochemistry for eNOS in lung sections showed that the monocrotaline-induced decrease in eNOS immunostaining was partly reversed by p.o or i.p. treatment with KMUP-1 (Figure 9B).

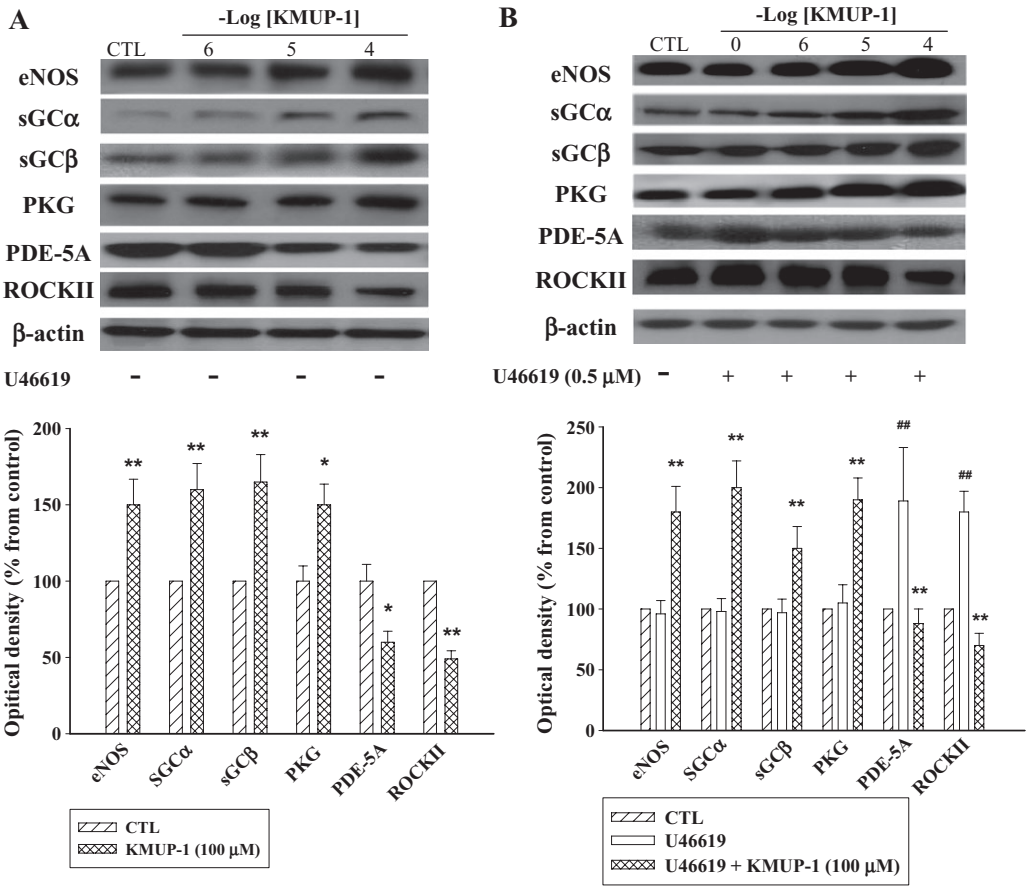
A
-Log [KMUP-1]
CTL
6
5
4
eNOS
sGCα
sGCβ
PKG
PDE-5A
ROCKII
β-actin
U46619
Opitical density (% from control)
eNOS
SGCα
sGCβ
PKG
PDE-5A
ROCKII
CTL
KMUP-1 (100 μM)
B
-Log [KMUP-1]
CTL
0
6
5
4
U46619 (0.5 μM)
Optical density (% from control)
CTL
U46619
U46619 + KMUP-1 (100 μM)

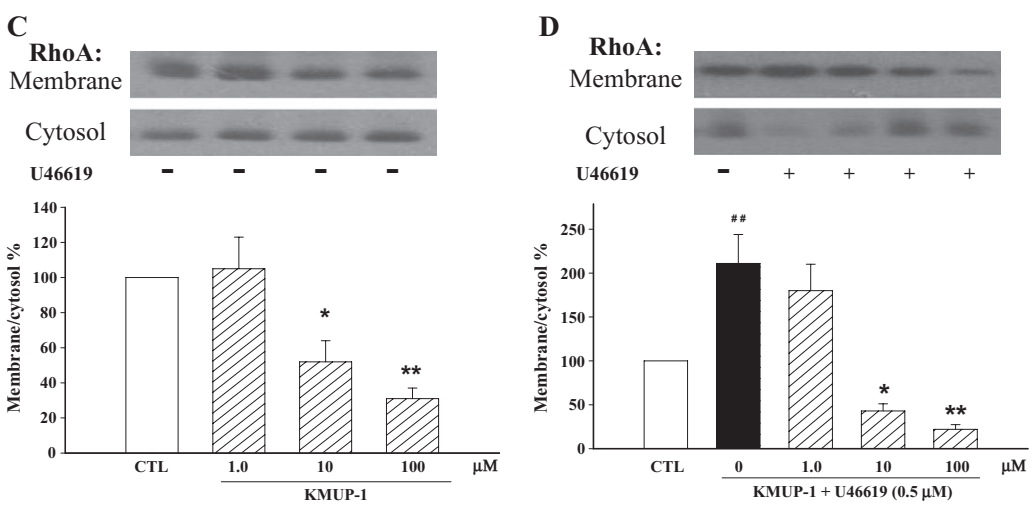
C
RhoA:
Membrane
Cytosol
U46619
Membrane/cytosol %
CTL
1.0
10
100
μM
KMUP-1
D
RhoA:
Membrane
Cytosol
U46619
Membrane/cytosol %
CTL
0
1.0
10
100
μM
KMUP-1 + U46619 (0.5 μM)

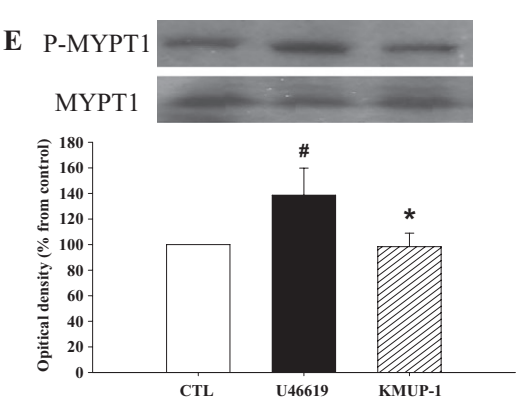
E
P-MYPT1
MYPT1
Optical density (% from control)
CTL
U46619
KMUP-1

Figure 3 Effects of U46619 on KMUP-1-induced expression of eNOS/sGC/PKG and inhibition of ROCK II/PDE-5A in isolated PA rings. KMUP-1 (1.0–100 μM) elevated eNOS/sGC/PKG and inhibited PDE-5A and ROCK II expression in isolated PA rings treated without (–)/(A) or with (+)/(B) U46619 (0.5 μM). (A) PA rings were incubated for 90 min with or without KMUP-1 in the absence of U46619; (B) PA rings were incubated for 60 min with or without KMUP-1, and then U46619 was added with for 30 min. Control was treated without KMUP-1. (C) KMUP-1 concentration-dependently inhibited RhoA activity in isolated PA rings in the absence of U46619; RhoA activity was represented by membrane/cytosol ratio of RhoA after treatment with KMUP-1 for 90 min. (D) Incubation of KMUP-1 with PA rings for 60 min, followed by U46619 (0.5 μM) for 30 min, concentration-dependently inhibited RhoA activity; (E) Rho kinase activity was quantified by the ratio of the amount of phosphorylated MYPT1 to total MYPT1 induced by U46619 (0.5 μM) and treatment with KMUP-1 (10 μM). $n = 6$. *$P < 0.05$; **$P < 0.01$ versus U46619; #$P < 0.05$; ##$P < 0.01$ versus control (CTL). eNOS, endothelial nitric oxide synthase; MYPT1, myosin phosphatase target subunit 1; PA, pulmonary artery; PDE-5A, phosphodiesterase-5A; PKG, protein kinase G; ROCK II, Rho kinase II; sGC, soluble guanylate cyclase.

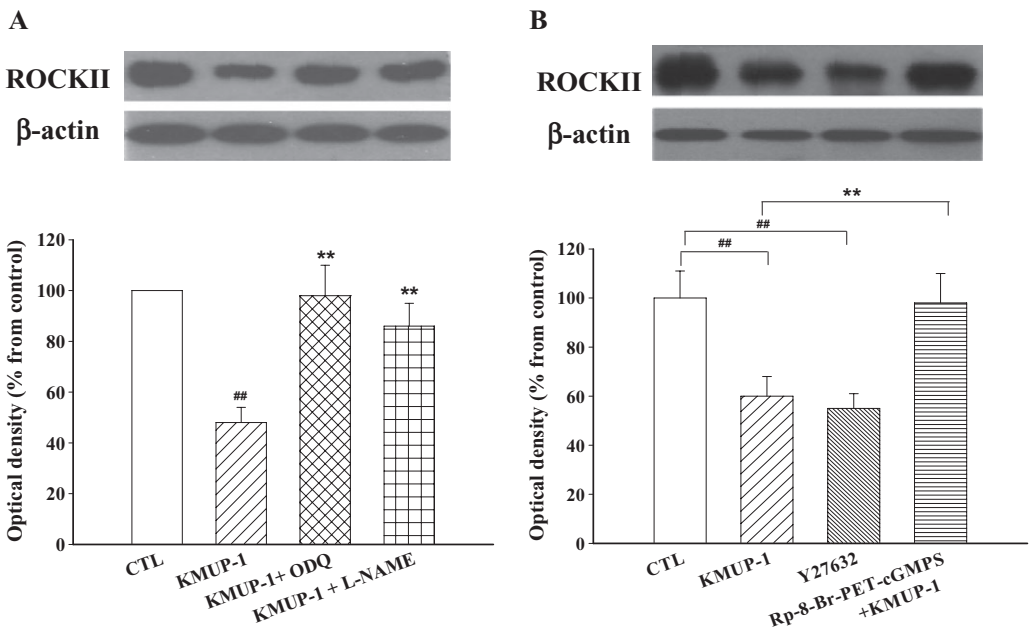

Figure 4 Effects of KMUP-1 and various pretreatments on expression of ROCK II in PA rings. (A) Pretreatment with ODQ (1 μM) and L-NAME (100 μM) for 10 min blocked the KMUP-1 (100 μM)-induced reduction of ROCK II in PA rings; (B) both KMUP-1 (10 μM) and Y27632 (10 μM) inhibited ROCK II expression in PA rings; pretreatment with Rp-8-Br-PET-cGMPS (0.01 μM) reversed KMUP-1-induced reduction of ROCK II. $n = 6$. **$P < 0.01$ versus KMUP-1; ##$P < 0.01$ versus control (CTL). L-NAME, N^{ω}-nitro-L-arginine methyl ester; ODQ, 1*H*-[1,2,4]oxadiazolo[4,3-*a*]quinoxalin-1-one; PA, pulmonary artery; ROCK II, Rho kinase II.

Discussion and conclusions

We have used KMUP-1 to inhibit PAH, induced either acutely with U46619 or chronically with monocrotaline. To elucidate the mechanism of action of KMUP-1, we compared the co-localized expression of eNOS, sGC, cGMP, PKG, PDE-5A and RhoA/ROCK II in PA and lung tissue before and after experimental treatment. To confirm that KMUP-1 can ameliorate vascular narrowing and RVH, we measured MPAP and RV/LV + S weight ratio as an index of RVH. We supported these findings by observing changes in PA wall thickness and immunostaining for eNOS in lung tissues. KMUP-1 relaxed phenylephrine- or U46619-constricted PA, enhanced eNOS, sGC and PKG, and inhibited PDE-5A, RhoA and ROCK II expression in the absence and presence of U46619. A scheme of the proposed mechanism of action by which KMUP-1 inhibits PAH is outlined in Figure 10. Raised levels of eNOS and decreased levels of RhoA/ROCK II following KMUP-1 is proposed to prolong vascular relaxation and reduce resistance, thus lessening PAH.

KMUP-1 increased basal cGMP and cAMP

KMUP-1 is known to block α_{1A}-adrenoceptors (Liu *et al.*, 2007), which is why KMUP-1 inhibited the α_1-adrenceptor agonist phenylephrine-induced PA constriction. KMUP-1 inhibited constriction in both phenylephrine and U46619-contracted PA rings, indicating that it works via both NO/cGMP-dependent RhoA/ROCK II suppression and α_{1A}-adrenoceptor blockade. However, ODQ, L-NAME and SQ22536 all reversed KMUP-1-induced relaxation, indicating that NO/sGC/cGMP and adenyl cyclase/cAMP signalling were also involved in relaxing the PA. In plasma from U46619-treated rats, KMUP-1 increased basal cGMP almost threefold compared with cAMP, indicating the predominant involvement of cGMP, although there were no significant differences between cGMP and cAMP.

KMUP-1-induced Ca^{2+} desensitization

RhoA/ROCK expression in PA smooth muscle is associated with vascular resistance caused by Ca^{2+} sensitization, which

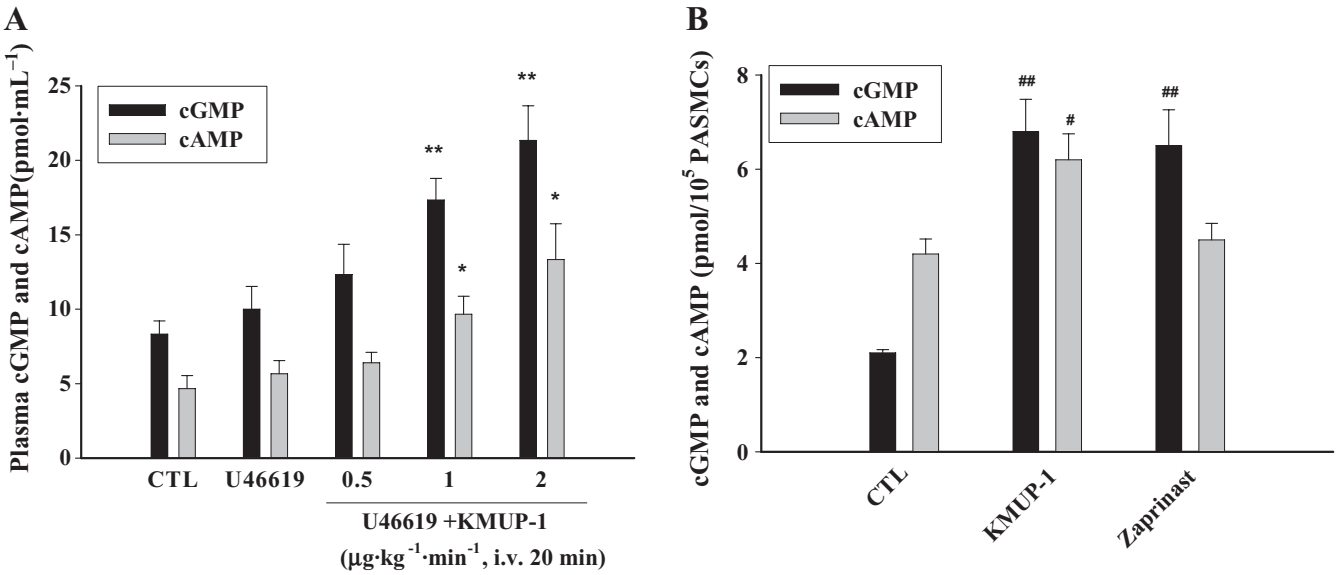

Figure 5 Effects of KMUP-1 on cGMP and cAMP. (A) Effects of intravenous KMUP-1 (0.5, 1, 2 μg·kg^{-1}·min^{-1}, 20 min) on plasma cAMP and cGMP after intravenous infusion of U46619 (2.5 μg·kg^{-1}·min^{-1}, 30 min); (B) effects of KMUP-1 (10 μM) and zaprinast (10 μM) on production of cGMP and cAMP in cultured PASMCs. Values are expressed as means ± s.e., $n = 6$. *$P < 0.05$; **$P < 0.01$ versus U46619; # $P < 0.05$; ##$P < 0.01$ versus control (CTL). PASMCs, pulmonary artery smooth muscle cells.

regulates pulmonary vascular tone (Sauzeau *et al*., 2000). KMUP-1 inhibited the expression of ROCK II, suggesting that Ca^{2+} desensitization might be related to reductions in vascular resistance. Resting and ANG II-induced levels of $[Ca^{2+}]_i$ were higher in PA myocytes cultured from pulmonary hypertensive rats than in those cultured from normotensive ones (Li *et al*., 1997). Sildenafil was found to increase cGMP and alter calcium signalling in PA myocytes (Pauvert *et al*., 2004). In our experiments, KMUP-1 reduced ANG II-induced increase of extracellular $[Ca^{2+}]_i$ and inhibited TG-induced Ca^{2+} efflux from the ER, similarly to sildenafil, inhibiting Ca^{2+} mobilization in PASMCs. Thus, KMUP-1 inhibited both intracellular Ca^{2+} mobilization and Ca^{2+} sensitization in PASMCs.

KMUP-1 up-regulated eNOS, down-regulated ROCK and phosphorylated MYPT1

Co-localized protein expression indicated that KMUP-1 increased eNOS, sGC and cGMP, decreased PDE-5A and ROCK II expression, and phosphorylated MYPT-1 in PA. The action of KMUP-1 in the presence of U46619 involved the upstream expression of eNOS and sGC, reduction of cGMP-specific PDE and downstream inhibition of ROCK II, characterized by increased PKG and plasma cGMP. We confirmed that KMUP-1 simultaneously increased eNOS, decreased ROCK II and phosphorylated MYPT-1 in the presence of U46619. KMUP-1 inhibited ROCK II expression, similar to the effects of the ROCK inhibitor, Y27632. The expression of ROCK in PA was diminished by both the eNOS inhibitor L-NAME and the sGC inhibitor ODQ, and was reversed by pretreatment with a PKG inhibitor Rp-8-Br-PET-cGMPS, indicating the co-localization of ROCK II, sGC and PKG expression in PA. These findings indicated the existence of a NO/sGC/cGMP-dependent ROCK inhibition pathway.

Inhibition of RhoA/ROCK expression attenuates PAH by inhibiting vasoconstriction and proliferation (Abe *et al*., 2004; Nagaoka *et al*., 2005). In contrast, eNOS allows the local regulation of vascular smooth muscle tone and cell proliferation by inhibiting expression of ROCK. Thus, eNOS and ROCK act in an opposing, regulatory relationship (Takemoto *et al*., 2002). The reduction of eNOS in monocrotaline-treated lung tissue was accompanied by increased RhoA/ROCK, indicating that eNOS reduction was mediated by increased ROCK and suggesting that ROCK inhibition may be useful to treat monocrotaline-induced PAH. Therefore, chronic administration of KMUP-1 reduced monocrotaline-induced PAH and its pathological consequences by maintaining raised levels of eNOS and suppressing RhoA/ROCK II expression.

PAH is caused in part by impairment of PKG, which is a downstream signalling component of the cGMP pathway, and up-regulation of ROCK blocks PKG-induced vasodilatation in PAH. We found that the PKG inhibitor Rp-8-Br-PET-cGMPS decreased KMUP-1-induced inhibition of ROCK II in PASMCs, indicating that KMUP-1 inhibited the expression of ROCK II, via effects on PKG. Notably, RhoA activity, represented by translocation from cytosol to cell membrane, was inhibited by KMUP-1 in monocrotaline-treated lung tissue and U46619-treated PA rings, suggesting a relationship between RhoA and PKG in the cGMP pathway.

eNOS and PDE-5A

It is less clear whether cGMP enhancement results from improved expression of eNOS or inhibition of PDE-5A. In our study, KMUP-1 inhibited PDE-5A expression in PA rings in the absence and presence of U46619. Inhibition of U46619-induced up-regulation of PDE-5A by KMUP-1 certainly leads to cGMP accumulation in plasma and PASMCs. However, in

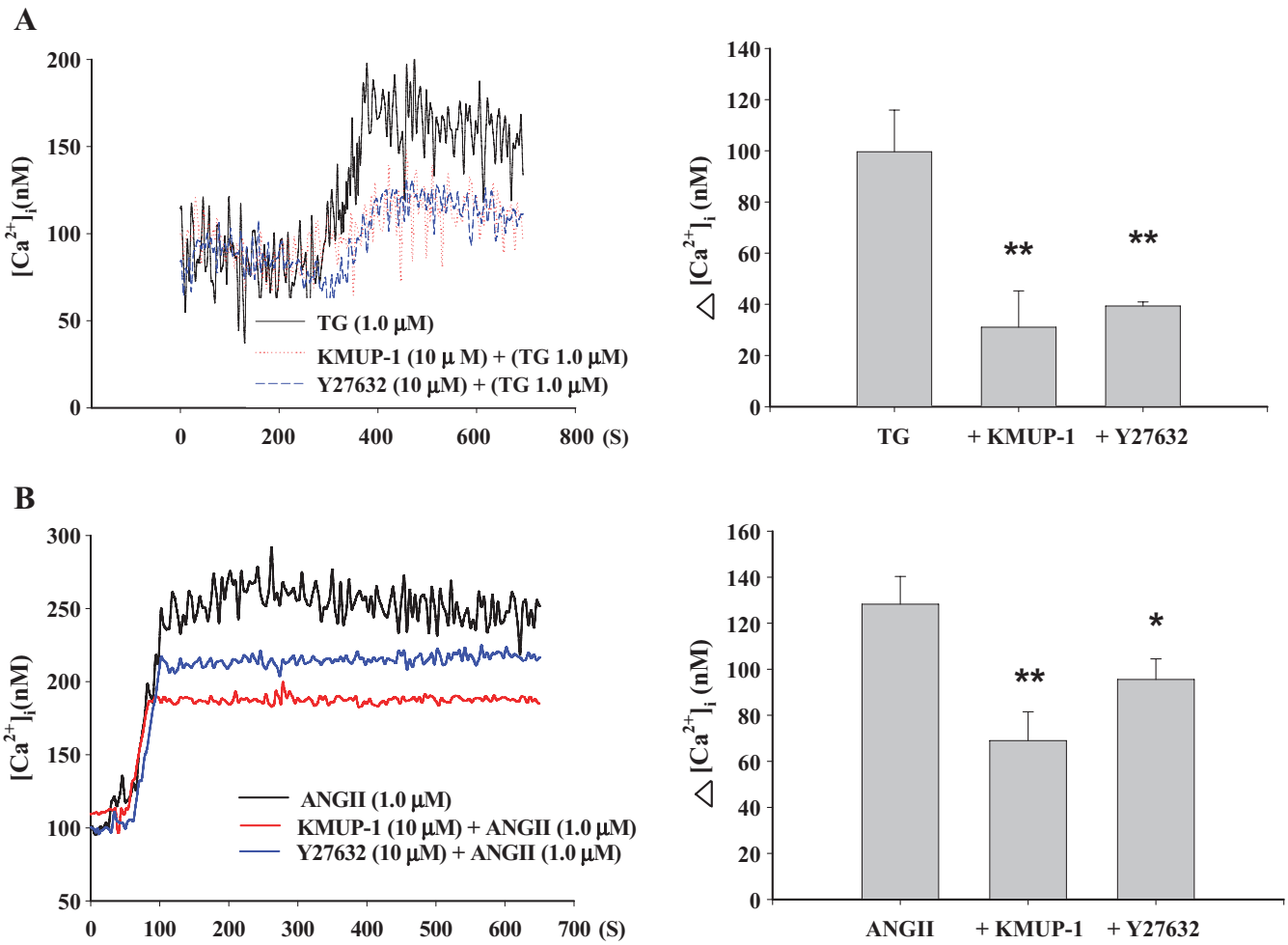

Figure 6 Effects of KMUP-1 and Y-27632 on $[Ca^{2+}]i$. KMUP-1 (10 μM) or Y27632 (10 μM) was added to cuvettes to inhibit the effects of thapsigargin (TG, 1.0 μM) (A) or angiotensin II (ANG II, 1.0 μM) (B) on increases of $[Ca^{2+}]_i$. $n = 4$. △ $[Ca^{2+}]_i$ indicated the difference in $[Ca^{2+}]_i$ between basal and peak levels elevated by TG or ANG II respectively. *$P < 0.05$; **$P < 0.01$ versus TG or ANG II.

monocrotaline-treated lung tissue, PDE-5A expression was not inhibited by KMUP-1. This difference may be due to different pathogenic mechanisms, including complex involvement of PDE-5A and isoforms released from multiple lung cells (Guazzi and Samaja, 2007). PDE-5A up-regulation was the most intensive signalling caused by acute application of U46619. RhoA expression/activity was the most intensive signalling caused by monocrotaline treatment. Neither KMUP-1 nor sildenafil could inhibit the monocrotaline-induced increases in PDE-5A expression. These findings indicate that enhanced eNOS expression is more important than PDE-5A suppression for inhibiting PAH.

Endothelial eNOS function

How eNOS functions in the endothelium is a major focus of our study. Acute hypoxia might be related to vasoconstriction. Raising eNOS expression should reverse hypoxia-induced endothelium dysfunction and vasoconstriction. However, hypoxia produced megalocytosis and Golgi blockade of endothelial cells, leading to the sequestration of eNOS away from caveolar locations and providing a mechanism for the often-reported reduction of NO in PAH (Mukhopadhyay *et al*., 2007). How KMUP-1 may sustain higher levels of eNOS, reducing hypoxia-induced megalocytosis and Golgi blockade, is still unclear (Mukhopadhyay *et al*., 2008).

Blood oxygenation

Intravenous U46619 lowers blood oxygen and induces acute PAH, which is characterized by increased contractility and resistance of PA, decreased local NO, up-regulated ROCK and Ca^{2+} sensitization, and increased arterial $[Ca^{2+}]_i$ in PA (Losapio *et al*., 2005). As mitochondria can act as oxygen sensors, a dysfunction of the mitochondrial respiratory chain could be related to hypoxic pulmonary vasoconstriction (Weissmann *et al*., 2003). The link between changes in the mitochondrial respiratory chain and reduced PO_2 in KMUP-1-treated PAH should be investigated further.

An important concern in the treatment of PAH is the increased oxygen consumption and increased levels of cAMP, causing unwanted cardiac overloading. However, KMUP-1 inhibited cAMP-enhancing isoprenaline-induced cardiac hypertrophy (Yeh *et al*., 2010). In the present study, KMUP-1

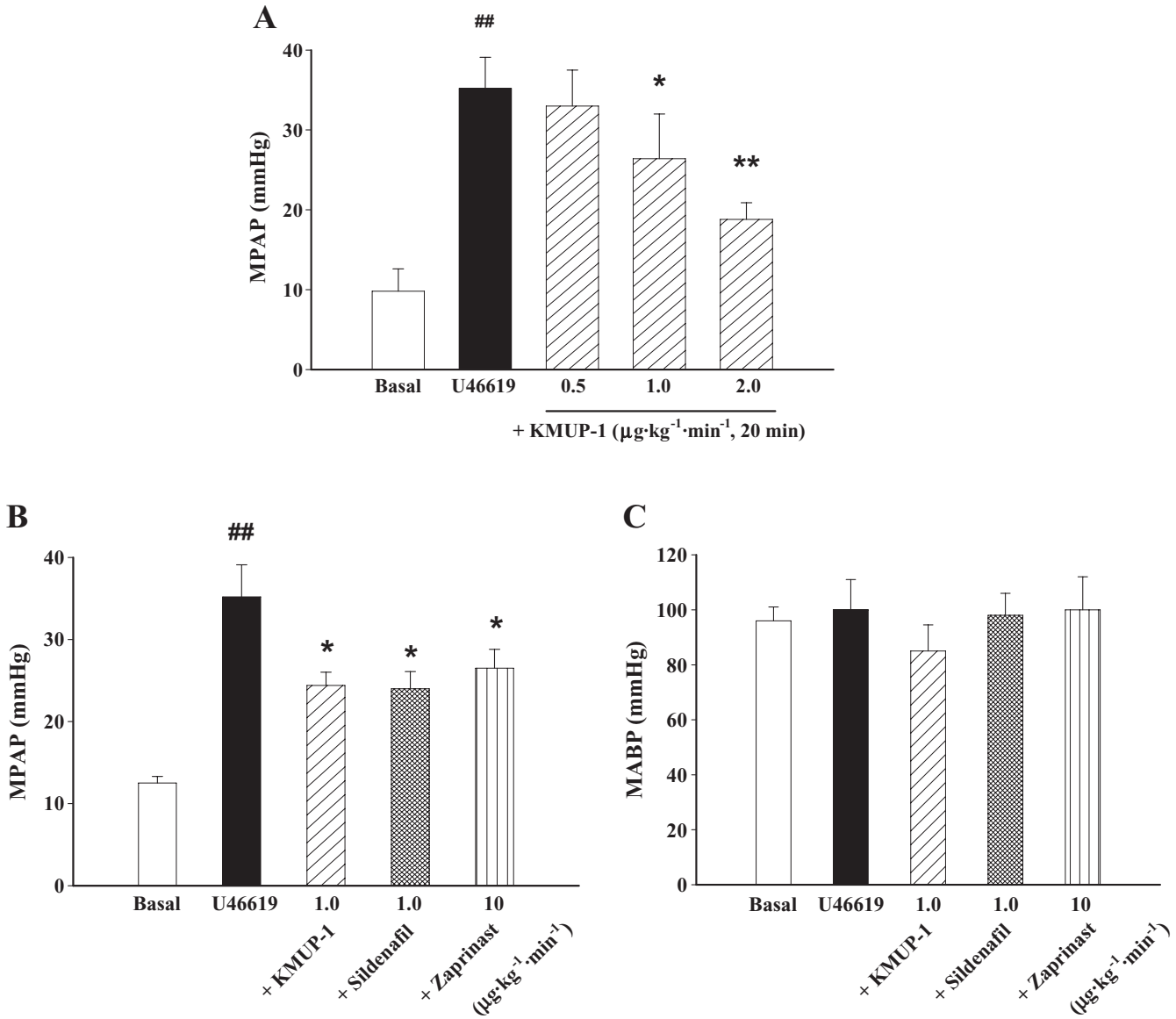

Figure 7 Inhibition of MPAP and MABP by KMUP-1. (A) Pretreatment with KMUP-1 (0.5–2.0 μg·kg^{-1}·min^{-1}, 20 min, i.v.) reduced U46619 (2.5 μg·kg^{-1}·min^{-1}, 30 min, i.v.)-induced increases in MPAP; (B) KMUP-1 (1.0 μg·kg^{-1}·min^{-1}), sildenafil (1.0 μg·kg^{-1}·min^{-1}) and zaprinast (10 μg·kg^{-1}·min^{-1}) were intravenously pre-infused for 20 min to inhibit U46619 (2.5 μg·kg^{-1}·min^{-1}, 30 min, i.v.)-induced MPAP; (C) effects of KMUP-1 (1.0 μg·kg^{-1}·min^{-1}, i.v.), sildenafil (1.0 μg·kg^{-1}·min^{-1}, i.v.) and zaprinast (10 μg·kg^{-1}·min^{-1}, i.v.) on MABP after U46619 (2.5 μg·kg^{-1}·min^{-1}, 30 min, i.v.). The infusion of U46619 alone did not change MABP, and none of the pretreatments (KMUP-1, 1.0 μM; sildenafil, 1.0 μM; zaprinast, 10 μM) affected MABP during U46619 infusion. Values are expressed as means ± s.e, $n = 6$, *$P < 0.05$; **$P < 0.01$ versus U46619, ##$P < 0.01$ versus control. Black column indicates U46619 infusion without treatment. MABP, mean arterial blood pressure; MPAP, mean pulmonary artery pressure.

Table 2 Effects of KMUP-1, sildenafil and zaprinast on blood oxygenation during hypoxia induced by infusion of U46619 in rats

	Control	*U46619*	*KMUP-1 + U46619*	*Sildenafil + U46619*	*Zaprinast + U46619*
PO_2	103.2 ± 10.4	89.3 ± 3.1#	100.1 ± 2.2*	100.6 ± 3.0*	98.5 ± 3.1*

Data in the table are means ± s.e., $n = 6$. U46619 was infused at 2.5 μg·kg^{-1}·min^{-1}, i.v. for 30 min and blood samples taken from the femoral artery at the end of the infusion.
*$P < 0.05$ versus U46619, #$P < 0.05$ versus control values.

Table 3 Effects of KMUP-1 on monocrotaline-induced changes in MABP, HR, MPAP, RV/LV + S ratio and PA wall thickness

Treatment	*MABP (mmHg)*	*HR (bpm)*	*MPAP (mmHg)*	*RV/LV + S (%)*	*Wall thickness (%)*
Control	114.5 ± 6.4	365 ± 20	12.3 ± 1.2	21.4 ± 0.4	26.9 ± 2.7
Monocrotaline	102.5 ± 8.2	344 ± 18	30.7 ± 1.2$^{\#\#}$	44.8 ± 1.0$^{\#\#}$	59.9 ± 12.7$^{\#}$
KMUP-1					
5 mg·kg^{-1}, p.o.	104.4 ± 5.4	342 ± 12	21.8 ± 2.9*	31.5 ± 0.7*	30.7 ± 8.6*
1 mg·kg^{-1}, i.p.	100.2 ± 4.0	384 ± 17	18.7 ± 4.6*	35.8 ± 1.0*	40.8 ± 3.5*

Data in the table are means ± s.e. of $n = 6$. *$P < 0.05$ versus monocrotaline; $^{\#}P < 0.05$, $^{\#\#}P < 0.01$ versus control.
Twenty-one days after monocrotaline injection (i.p.), rats were anaesthetized; MABP, HR and MPAP were measured and then samples were taken for analysis. KMUP-1 or vehicle was given daily for 21 days after monocrotaline.
HR, heart rate; MABP, mean arterial blood pressure; MPAP, mean pulmonary artery pressure; PA, pulmonary artery; RV/LV + S, weight ratio of right ventricular wall area to left ventricular wall area plus septum.

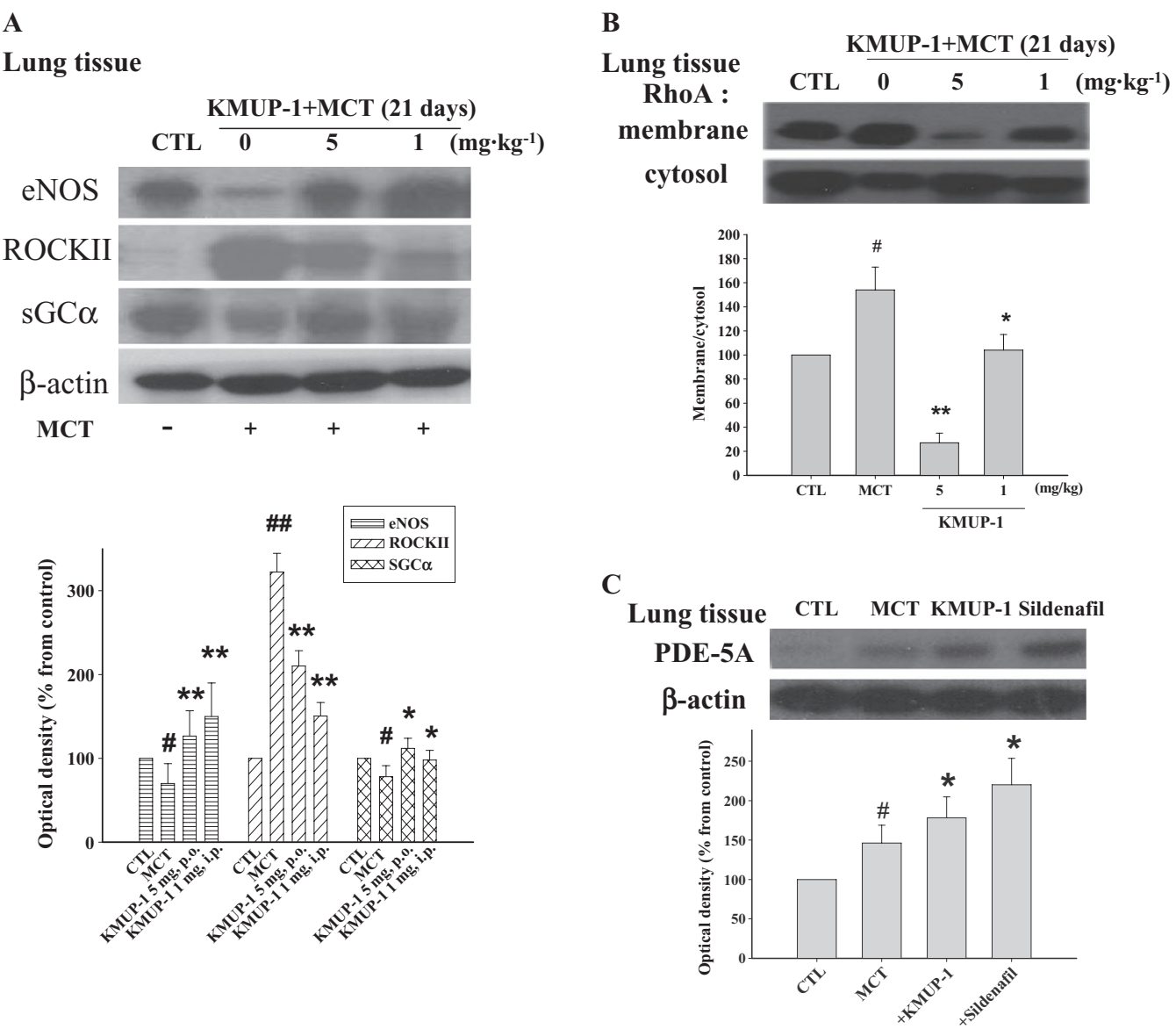

Figure 8 Effects of KMUP-1 on monocrotaline (MCT)-induced expressions of eNOS, sGC, ROCK II, RhoA and PDE-5A in lung tissue. (A) KMUP-1 (5 mg·kg^{-1}, p.o. or 1 mg·kg^{-1}, i.p., 21 days) increased eNOS and sGC, and decreased ROCK II expression in MCT-treated rat lung tissues on day 21; (B) KMUP-1 (5 mg·kg^{-1}, p.o. or 1 mg·kg^{-1}, i.p. for 21 days) decreased RhoA activity, represented by membrane/cytosol ratio, in MCT-treated rat lung tissues on day 21; (C) effects of KMUP-1 and sildenafil at 5 mg·kg^{-1}·day^{-1} on MCT-induced PDE-5A expression in lung tissue on day 21. Values are expressed as means ± s.e. of $n = 6$. *$P < 0.05$; **$P < 0.01$ versus MCT; #$P < 0.05$; ##$P < 0.01$ versus control (CTL). + and –, administration with and without MCT; eNOS, endothelial nitric oxide synthase; +KMUP-1 and +sildenafil, administration of KMUP-1 and sildenafil in MCT-treated animals respectively; PDE-5A, phosphodiesterase-5A; ROCK II, Rho kinase II; sGC, soluble guanylate cyclase.

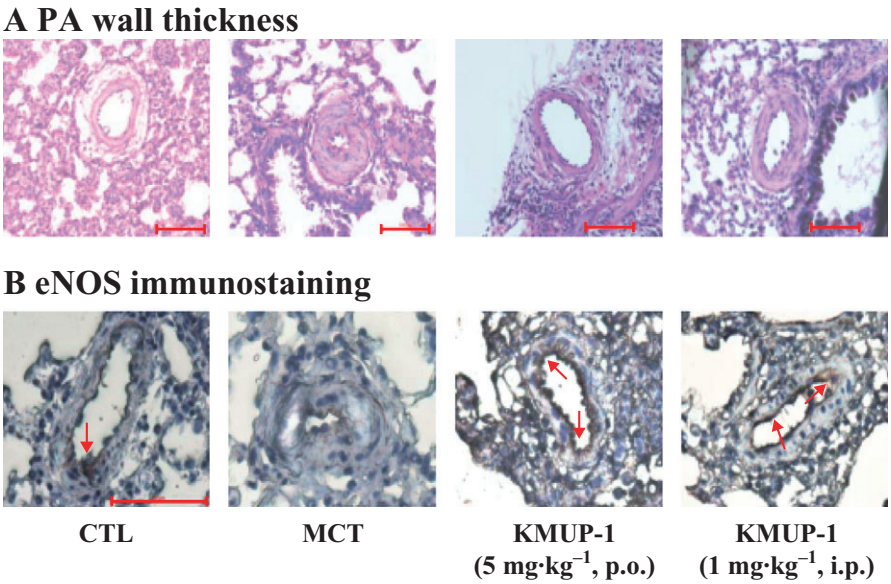

Figure 9 Microphotographs showing effects of KMUP-1 on monocrotaline (MCT)-induced vascular remodelling and eNOS immunostaining of PA in lung sections. (A) Microphotographs of PA stained by haematoxylin and eosin in section of lungs from rats treated with MCT and KMUP-1; (B) eNOS immunostaining in PA rings shown in brown colour. The arrowheads represent positive staining. Scale bar = 100 μm. PA, pulmonary artery.

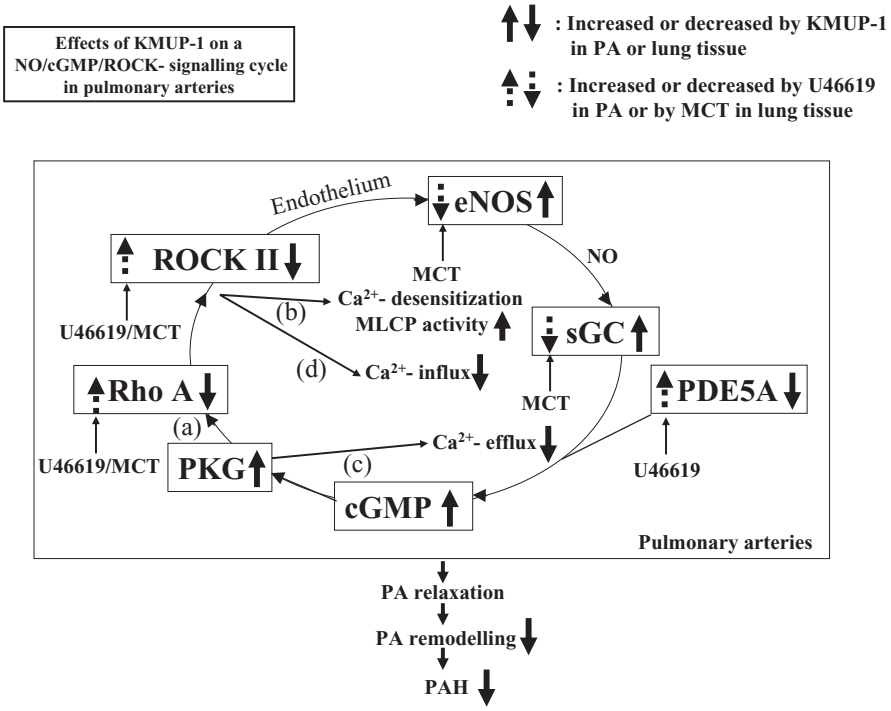

Figure 10 Proposed mechanism of inhibition by KMUP-1 on PAH. Activation of eNOS and sGC in pulmonary arterial (PA) endothelium and inhibition of RhoA/ROCK II and PDE-5A in PA smooth muscle cells by KMUP-1 reverses U46619-induced acute PAH and protects against monocrotaline (MCT)-induced chronic PAH over long-term administration. Inhibition of endothelial RhoA/ROCK by KMUP-1 can initiate eNOS expression. PKG, increased by KMUP-1-induced enhancement of eNOS, activation of sGC and inhibition of PDE-5A, phosphorylates RhoA (a) and interferes with ROCK II inhibition of MLCP, increasing MLCP activity. Thus, MLCP dephosphorylates MLC and enhances smooth muscle relaxation, showing Ca^{2+} desensitization (b); TG induces Ca^{2+} release (Ca^{2+} efflux) from ER (c) and reduces $[Ca^{2+}]_i$, thus inhibiting MLC kinase (MLCK) and vasoconstriction; inhibition of ROCK II by KMUP-1 and Y27632 reduces ANG II-induced Ca^{2+} influx in PASMCs, indicating Ca^{2+} entry blocking activity (d) in PASMCs. Inhibition of ROCK II by KMUP-1 in endothelium can increase eNOS, repeating a cycle of eNOS activation/ROCK II inhibition signalling during long-term administration. ANG II, angiotensin II; eNOS, endothelium nitric oxide synthase; ER, endoplasmic reticulum; MLCP, 'phosphatase; PAH, pulmonary artery hypertension; PASMCs, pulmonary artery smooth muscle cells; PDE-5A, phosphodiesterase-5A; PKG, protein kinase G; ROCK, Rho kinase; ROCK II, Rho kinase II; sGC, soluble guanylate cyclase; TG, thapsigargin.

increased eNOS expression to elevate pulmonary cGMP levels, confirming earlier results (McNamara *et al*., 2006). These facts indicate that KMUP-1 might reduce the risk of hypoxia by increasing blood oxygenation and plasma cGMP. The PDE-5 inhibitor zaprinast also increased cGMP, but not cAMP, reversing U46619-induced lowering of blood oxygenation.

KMUP-1 combines the effects of sildenafil, ROCK inhibitors and statins

Sildenafil, ROCK inhibitors and statins have been used for inhibiting PAH. Similarly to sildenafil, KMUP-1 inhibited PAH by a cGMP-dependent pathway. Like the ROCK inhibitors Y27632 and fasudil, KMUP-1 displayed RhoA/ROCK inactivation and Ca^{2+} desensitization activities. Similar to statins, KMUP-1 may increase eNOS mRNA stability by inhibiting endothelial Rho GTPase, leading to increased bioavailability of endothelium-derived NO (Rikitake and Liao, 2005; Kosmidou *et al*., 2007). Inhibition of PAH by KMUP-1 thus combines the benefits of three standard drugs in one compound.

Metabolic interference by monocrotaline

The effects of KMUP-1 *in vivo* may be subject to possible metabolic interference by monocrotaline. Indeed, injection of monocrotaline without KMUP-1 increased expression of PDE-5A and RhoA/ROCK II, and reduced expression of eNOS, sGC and PKG. Starting treatment with KMUP-1 at different times after monocrotaline might change the metabolism of monocrotaline in liver, affecting the effectiveness of KMUP-1. The relationship between protein expression and this form of metabolic interference remains to be investigated.

Animal models of PAH

In acute PAH, KMUP-1 significantly altered eNOS, ROCK and PDE-5A expression within 120 min in a time-dependent manner, indicating a rapid response to protect against U46619-induced acute or hypoxic protein expression. In chronic PAH, the monocrotaline/rat model does not develop the occlusive neointimal and plexiform lesions that are characteristic of human severe PAH (Ivy *et al*., 2005). In another experimental model, aortic banding in rats, there are changes of protein expression in the PA (Tan *et al*., 2006). The model of PAH induced by hypoxia in rats is closer to human PAH, and this model will be investigated in the future.

In conclusion, KMUP-1 inhibited U46619-induced acute PAH, by increasing eNOS and suppressing RhoA/ROCK, and reversed monocrotaline-induced chronic PAH, mediated via eNOS down-regulation and RhoA/ROCK II up-regulation (Figure 10). We suggest that the increase of eNOS by KMUP-1 leads to increased NO, generating a cGMP-dependent inhibition of RhoA/ROCK II and Ca^{2+} desensitization in PASMCs. Treatment with KMUP-1 might therefore be able to reduce vascular resistance, hyperplasia and RVH in PAH.

However we are aware of the unwanted fall in MABP that could result from reduced RhoA and increased eNOS activity (Masumoto *et al*., 2001; Ito *et al*., 2003; Tölle *et al*., 2006). KMUP-1 has activated the NO/cGMP pathway in rat aortic tissue and has produced hypotension (Wu *et al*., 2001). Further investigation into the effects of KMUP-1 in PAH induced by hypoxia and aortic banding should be pursued in future studies.

Acknowledgement

This work was supported by the National Science Council of Taiwan grants NSC 94-2323-B-037-005 and NSC 95-2323-B-037-004.

Conflicts of interest

None.

References

Abe K, Shimokawa H, Morikawa K, Uwatoku T, Oi K, Matsumoto Y *et al*. (2004). Long-term treatment with a Rho-kinase inhibitor improves monocrotaline-induced fatal pulmonary hypertension in rats. *Circ Res* **94**: 385–393.

Alexander SPH, Mathie A, Peters JA (2009). Guide to receptors and channels (GRAC), 4th edn. *Br J Pharmacol* **158** (Suppl. 1): S1–S254.

Bohm F, Pernow J (2007). The importance of endothelin-1 for vascular dysfunction in cardiovascular disease. *Cardiovasc Res* **76**: 8–18.

Cogolludo A, Moreno L, Bosca L, Tamargo J, Perez-Vizcaino F (2003). Thromboxane A2-induced inhibition of voltage-gated K^+ channels and pulmonary vasoconstriction: role of protein kinase Czeta. *Circ Res* **93**: 656–663.

Copple BL, Ganey PE, Roth RA (2003). Liver inflammation during monocrotaline hepatotoxicity. *Toxicology* **190**: 155–169.

Deruelle P, Grover TR, Storme L, Abman SH (2005). Effects of BAY 41-2272, a soluble guanylate cyclase activator, on pulmonary vascular reactivity in the ovine fetus. *Am J Physiol Lung Cell Mol Physiol* **288**: L727–L733.

Feng J, Ito M, Ichikawa K, Isaka N, Nishikawa M, Hartshorne DJ *et al*. (1999). Inhibitory phosphorylation site for Rho-associated kinase on smooth muscle myosin phosphatase. *J Biol Chem* **274**: 37385–37390.

Fukumoto Y, Matoba T, Ito A, Tanaka H, Kishi T, Hayashidani S *et al*. (2005). Acute vasodilator effects of a Rho-kinase inhibitor, fasudil, in patients with severe pulmonary hypertension. *Heart* **91**: 391–392.

Gao Y, Portugal AD, Negash S, Zhou W, Longo LD, Usha Raj J (2007). Role of Rho kinases in PKG-mediated relaxation of pulmonary arteries of fetal lambs exposed to chronic high altitude hypoxia. *Am J Physiol Lung Cell Mol Physiol* **292**: L678–L684.

Guazzi M, Samaja M (2007). The role of PDE5-inhibitors in cardiopulmonary disorders: from basic evidence to clinical development. *Curr Med Chem* **14**: 2181–2191.

Homma N, Nagaoka T, Karoor V, Imamura M, Taraseviciene-Stewart L, Walker LA *et al*. (2008). Involvement of RhoA/Rho kinase signaling in protection against monocrotaline-induced pulmonary hypertension in pneumonectomized rats by dehydroepiandrosterone. *Am J Physiol Lung Cell Mol Physiol* **295**: L71–L78.

Homma N, Nagaoka T, Morio Y, Ota H, Gebb SA, Karoor V *et al*. (2007). Endothelin-1 and serotonin are involved in activation of RhoA/Rho kinase signaling in the chronically hypoxic hypertensive rat pulmonary circulation. *J Cardiovasc Pharmacol* **50**: 697–702.

Hongo M, Ryoke T, Schoenfeld J, Hunter J, Dalton N, Clark R *et al*. (2000). Effects of growth hormone on cardiac dysfunction and gene expression in genetic murine dilated cardiomyopathy. *Basic Res Cardiol* **95**: 431–441.

Ito K, Hirooka Y, Sakai K, Kishi T, Kaibuchi K, Shimokawa H *et al*. (2003). Rho/Rho-kinase pathway in brain stem contributes to blood pressure regulation via sympathetic nervous system: possible involvement in neural mechanisms of hypertension. *Circ Res* **92**: 1337–1343.

Ivy DD, McMurtry IF, Colvin K, Imamura M, Oka M, Lee DS *et al*. (2005). Development of occlusive neointimal lesions in distal pulmonary arteries of endothelin B receptor-deficient rats: a new model of severe pulmonary arterial hypertension. *Circulation* **111**: 2988–2996.

Kirsch M, Kemp-Harper B, Weissmann N, Grimminger F, Schmidt HH (2008). Sildenafil in hypoxic pulmonary hypertension potentiates a compensatory up-regulation of NO-cGMP signaling. *FASEB J* **22**: 30–40.

Korn C, Scholz SR, Gimadutdinow O, Lurz R, Pingoud A, Meiss G (2005). Interaction of DNA fragmentation factor (DFF) with DNA reveals an unprecedented mechanism for nuclease inhibition and suggests that DFF can be activated in a DNA-bound state. *J Biol Chem* **280**: 6005–6015.

Kosmidou I, Moore JP, Weber M, Searles CD (2007). Statin treatment and 3′ polyadenylation of eNOS mRNA. *Arterioscler Thromb Vasc Biol* **27**: 2642–2649.

Lamberts RR, Caldenhoven E, Lansink M, Witte G, Vaessen RJ, St Cyr JA *et al*. (2007). Preservation of diastolic function in monocrotaline-induced right ventricular hypertrophy in rats. *Am J Physiol Heart Circ Physiol* **293**: H1869–H1876.

Li Z, Zhang Q, Zhao S, Wei M, Cong H, Ouda H *et al*. (1997). High responsiveness of cytosolic free calcium concentration to angiotensin II in cultured pulmonary arterial myocytes from pulmonary hypertensive rats. *Res Commun Mol Pathol Pharmacol* **97**: 125–130.

Liu CM, Lo YC, Wu BN, Wu WJ, Chou YH, Huang CH *et al*. (2007). cGMP-enhancing- and alpha1A/alpha1D-adrenoceptor blockade-derived inhibition of Rho-kinase by KMUP-1 provides optimal prostate relaxation and epithelial cell anti-proliferation efficacy. *Prostate* **67**: 1397–1410.

Losapio JL, Sprague RS, Lonigro AJ, Stephenson AH (2005). 5, 6-EET-induced contraction of intralobar pulmonary arteries depends on the activation of Rho-kinase. *J Appl Physiol* **99**: 1391–1396.

Masumoto A, Hirooka Y, Shimokawa H, Hironaga K, Setoguchi S, Takeshita A (2001). Possible involvement of Rho-kinase in the pathogenesis of hypertension in humans. *Hypertension* **38**: 1307–1310.

McLaughlin VV, McGoon MD (2006). Pulmonary arterial hypertension. *Circulation* **114**: 1417–1431.

McNamara PJ, Laique F, Muang-In S, Whyte HE (2006). Milrinone improves oxygenation in neonates with severe persistent pulmonary hypertension of the newborn. *J Crit Care* **21**: 217–223.

Mukhopadhyay S, Lee J, Sehgal PB (2008). Depletion of the ATPase NSF from Golgi membranes with hypo-S-nitrosylation of vasorelevant proteins in endothelial cells exposed to monocrotaline pyrrole. *Am J Physiol Heart Circ Physiol* **295**: H1943–H1955.

Mukhopadhyay S, Xu F, Sehgal PB (2007). Aberrant cytoplasmic sequestration of eNOS in endothelial cells after monocrotaline, hypoxia, and senescence: live-cell caveolar and cytoplasmic NO imaging. *Am J Physiol Heart Circ Physiol* **292**: H1373–H1389.

Nagaoka T, Fagan KA, Gebb SA, Morris KG, Suzuki T, Shimokawa H *et al*. (2005). Inhaled Rho kinase inhibitors are potent and selective vasodilators in rat pulmonary hypertension. *Am J Respir Crit Care Med* **171**: 494–499.

Ni W, Geddes TJ, Priestley JR, Szasz T, Kuhn DM, Watts SW (2008). The existence of a local 5-hydroxytryptaminergic system in peripheral arteries. *Br J Pharmacol* **154**: 663–674.

Oka M, Homma N, Taraseviciene-Stewart L, Morris KG, Kraskauskas D, Burns N *et al*. (2007). Rho kinase-mediated vasoconstriction is important in severe occlusive pulmonary arterial hypertension in rats. *Circ Res* **100**: 923–929.

Pauvert O, Bonnet S, Rousseau E, Marthan R, Savineau JP (2004). Sildenafil alters calcium signaling and vascular tone in pulmonary arteries from chronically hypoxic rats. *Am J Physiol Lung Cell Mol Physiol* **287**: L577–L583.

Puchalski MD, Lozier JS, Bradley DJ, Minich LL, Tani LY (2006). Electrocardiography in the diagnosis of right ventricular hypertrophy in children. *Pediatrics* **118**: 1052–1055.

Rikitake Y, Liao JK (2005). Rho GTPases, statins, and nitric oxide. *Circ Res* **97**: 1232–1235.

Sauzeau V, Le Jeune H, Cario-Toumaniantz C, Smolenski A, Lohmann SM, Bertoglio J *et al*. (2000). Cyclic GMP-dependent protein kinase signaling pathway inhibits RhoA-induced Ca^{2+} sensitization of contraction in vascular smooth muscle. *J Biol Chem* **275**: 21722–21729.

Schach C, Xu M, Platoshyn O, Keller SH, Yuan JX (2007). Thiol oxidation causes pulmonary vasodilation by activating K^+ channels and inhibiting store-operated Ca2+ channels. *Am J Physiol Lung Cell Mol Physiol* **292**: L685–L698.

Takemoto M, Sun J, Hiroki J, Shimokawa H, Liao JK (2002). Rho-kinase mediates hypoxia-induced downregulation of endothelial nitric oxide synthase. *Circulation* **106**: 57–62.

Tan MS, Chai CY, Wu JR, Yeh JL, Chen IJ, Kwan AL *et al*. (2006). Differential change in expression of pulmonary ET-1 and eNOS in rats after chronic left ventricular pressure overload. *Exp Biol Med* **231**: 948–953.

Tölle M, Giebing G, Tietge UJ, Jankowski J, Jankowski V, Henning L *et al*. (2006). Diguanosine pentaphosphate: an endogenous activator of Rho-kinase possibly involved in blood pressure regulation. *J Hypertension* **24**: 1991–2000.

Wang J, Shimoda LA, Sylvester JT (2004). Capacitative calcium entry and TRPC channel proteins are expressed in rat distal pulmonary arterial smooth muscle. *Am J Physiol Lung Cell Mol Physiol* **286**: L848–L858.

Weissmann N, Ebert N, Ahrens M, Ghofrani HA, Schermuly RT, Hänze J *et al*. (2003). Effects of mitochondrial inhibitors and uncouplers on hypoxic vasoconstriction in rabbit lungs. *Am J Respir Cell Mol Biol* **29**: 721–732.

Wu BN, Chen CW, Liou SF, Yeh JL, Chung HH, Chen IJ (2006). Inhibition of proinflammatory tumor necrosis factor-a-induced inducible nitric-oxide synthase by xanthine-based 7-[2-[4-(2-chlorobenzene)piperazinyl]ethyl]-1,3-dimethylxanthine (KMUP-1) and 7 - [2 - [4 - (4 - nitrobenzene) piperazinyl] ethyl] - 1, 3 - dimethylxanthine (KMUP-3) in rat trachea: the involvement of soluble guanylate cyclase and protein kinase G. *Mol Pharmacol* **70**: 977–985.

Wu BN, Lin RJ, Lin CY, Shen KP, Chiang LC, Chen IJ (2001). A xanthine-based KMUP-1 with cyclic GMP enhancing and K^+ channels opening activities in rat aortic smooth muscle. *Br J Pharmacol* **134**: 265–274.

Yeh JL, Hsu JH, Wu PJ, Liou SF, Liu CP, Chen IJ *et al*. (2010). KMUP-1 attenuates isoproterenol-induced cardiac hypertrophy in rats through NO/cGMP/PKG and ERK1/2/calcineurin A pathways. *Br J Pharmacol* **159**: 1151–1160.